LAPEX EXPERIMENT : GENERAL DESCRIPTION AND POINTING ISSUES

A.Basili, G.Di Cocco, T. Franceschini, F. Frontera, L.A.Gizzi[@], G.Landini and S. Silvestri

I-TESRE, Area della Ricerca del CNR, Via Gobetti, 121, Bologna, Italy

[@]IFAM, Area della Ricerca del CNR, Via Moruzzi, 1, Pisa, Italy

***Abstract**: After the last flight of the LAPEX experiment, effort is being directed towards the a new generation of balloon experiments based upon long focal length (high angular resolution) X-ray telescopes [1]. The requirements of such telescopes in terms of pointing accuracy and stability are quite severe and require a complete redesign of the entire pointing system. To this purpose, the LAPEX platform is being gradually upgraded with the aim of developing a prototype of a high pointing performance system, HiPeG [2] ready to fly by middle 2002.*

1.Introduction

The aim of this document is to provide a summary of the performance of the original LAPEX experiment as obtained from the last flight (Fort Sumner, Oct.95) with emphasis on the pointing performance of the entire system. Also included in this report is a description of the LAPEX detector, a presentation of general flight information (altitude, position etc.), pre-flight operations (calibrations, background measurements and of azimuth pointing calibration) as well as a brief introduction to the scientific data collected.

2.The detector

The LAPEX detector is designed to perform spectral and temporal analysis of X-ray radiation emitted from X-ray sources in the 20-300 keV spectral range. The basic detection unit of the LAPEX experiment consists of a (145×145) mm^2 phoswich detector [3]. A phoswich detector consists of a sandwich of a 6 mm thick NaI(Tl) crystal optically coupled with a 50 mm thick CsI(Na) crystal. The phoswich is coupled to a photomultiplier tube that collects and amplifies the light pulses produced by the scintillation process in the crystal. In addition, an hexagonal tube rocking collimator with a field of view of 3 degrees (FWHM) is placed above the phoswich unit. Sixteen of these basic units are assembled in groups of four, enclosed in a box of plastic scintillator that acts as an active shield against charged particles. The basic detection principles of the LAPEX detector are described in **Fig.1**, where two of the sixteen units are shown along with the side-shields.

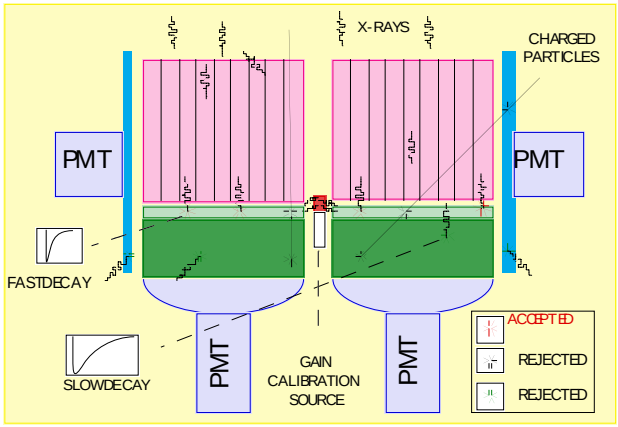

Fig.1. Schematic set-up of the LAPEX detector showing two of the sixteen detection units of the LAPEX detector. Each unit consists of a phoswich detector (see text) optically coupled to a photomultiplier tube.

Only events occurring in the NaI layer alone, characterised by a faster decay than those occurring in the CsI, are accepted by the on-

board electronic acquisition system. A schematic top-view of the final configuration is given in **Fig.2.** The detector is mounted on a gondola capable of azimuth-zenith tracking capability with an accuracy of ≈10 arcmin.

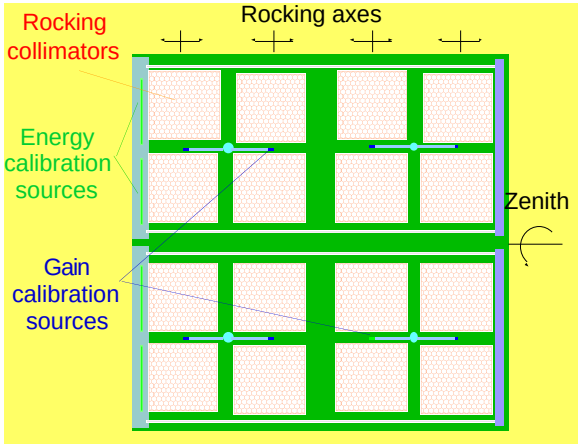

Fig.2. Top view of the LAPEX detector showing the sixteen collimators, the radioactive sources (Am241) employed for gain calibration and the four linear energy calibration sources (Ce139). The energy calibration arm was set to scan all units periodically during the flight in order to monitor the performance of the detector.

2.Gain and energy calibration

All the detection units are equipped with an automatic gain control (AGC) system based upon low intensity radioactive source of Am241 as shown schematically in **Fig.2**. These sources emit photons at 59.6 keV that are used by the feedback loop of the AGC to stabilise the gain of the units. The gain of each photomultiplier is set automatically by acting on the high voltage supply following a comparison between the amplitude of the pulse produced by each photon at 59.6 keV and a predefined level. The photon flux of the calibration source was adjusted in order to obtain an update frequency of the GC of approximately 2 Hz. The required flux was achieved by shielding the calibration source with the appropriate thickness of lead.

It should be pointed out that calibration photons can be discriminated by the detector and can be eventually subtracted. However, the identification process has a finite efficiency that changes from unit to unit. **Table.I** shows the percentage of gain calibration photons that are discriminated by the system.

D1:75%	D4:56%	C4:79%	C1:63%
D2:73%	D3:49%	C3:82%	C2:62%
A2:86%	A3:84%	B3:62%	B2:70%
A1:83%	A4:80%	B4:57%	B1:68%

Table.I. Fraction of the Am241 photons reaching the detector that are identified and can be subtracted from the actual data. The fraction is reported here for all the 16 units o the detector.

2.1 Pre-flight energy calibration

Each unit of the system was calibrated using a set of 8 different radioactive sources chosen in order to cover the whole spectral window of the detector as summarised in **Table.II**.

Source	Cd109	Ce139	Am241	Hg203	Cd109	Co57	Ce139	Hg203
E (keV)	22.5	34.0	59.6	74.5	88.0	122.1	165.8	279.2

Table.II. Radioactive sources and corresponding photon energies employed for the pre-flight energy calibration of the detector. The energy of the main spectral component for each source is shown here. The detailed structure of the emission spectrum of each source and the effect on the calibration will be discussed below.

The spectrum of each source for the 16 units was measured over a period of 1280 sec. The portion of the spectrum corresponding to the main spectral component of the calibration source was selected and fitted with a Gaussian profile, in order to determine the position (channel) of the peak and the corresponding energy resolution. In some cases (La-k emission @≈33 keV from Ce139), a blend of Gaussian functions was used in the fit in order to take

into account the detailed spectral structure of the emission. The energy calibration curve was obtained from a polynomial fit of data at a given photon energy. A simple quadratic function of the channel number was found to describe accurately the measured behaviour as summarised by the plots of **Fig.3a-d** where the calibration curves for each detector of the four units (A,B,C,D) are displayed.

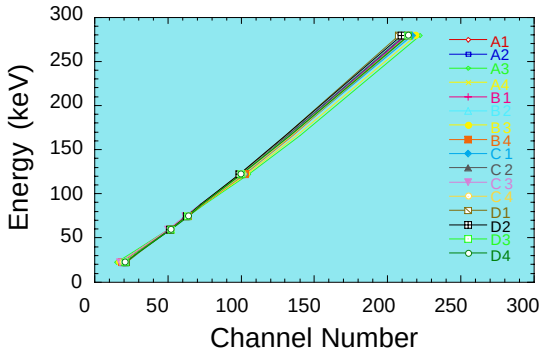

Fig.3. Pre-flight calibration curves of all the 16 detection units.

2.2 In-flight energy calibration

Energy calibration of all sixteen units was carried out by using on-board calibration sources consisting of four linear samples of Ce139 placed above the collimator plane, encapsulated in a motorised arm. The arm (see Fig.2) was set to scan all the units periodically during the flight in order to monitor the temporal stability of all the units. A spectrum of the calibration source was recorded approximately every hour and the main spectral component on the radiation detected, that is, the line at 165 keV was used as reference. The position of the peak was measured for the sequence of spectra for the 16 detectors and the result is shown in **Fig.4a-d.**

According to these plots, the fluctuation of the peak channel is stable within approximately ±5 channels, except in the case of unit D1 that shows a rapid shift of approximately 20 channels, early during the flight. However, later on, the system shows a behaviour similar to that of the other detectors.

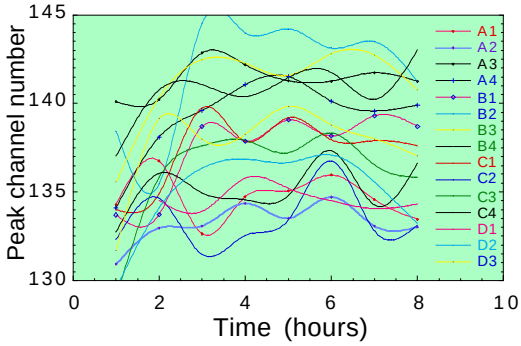

Fig.4. In-flight calibration of the 16 detection units showing the peak energy channel of the 165 keV from Ce139. Each data point refers to a calibration scan (see text) and the curves are a cubic spline fitting of the data.

3. Pointing system and calibration

As discussed above the LAPEX pointing is based upon a zenith-azimuth system. The azimuth motion is provided by a pivotal motion which acts on the entire gondola (see Fig.13) while the zenith motion acts on the detector modules only.

Fig.5. The 2000 kg LAPEX payload ready to fly from the NASA National Scientific Balloon Facility, NM. Clearly visible is the thermal shield all around the gondola and the pivot system for the azimuthal motion.

The zenithal motion is controlled by a 14-bit encoder which enables a pointing accuracy (with respect to the gondola horizontal plane) of ±0.6 arcmin. The primary azimuthal pointing system of the gondola is instead based upon techniques that exploit the earth magnetic field as relative reference direction. The absolute pointing is then recovered by taking into account the local magnetic declination.

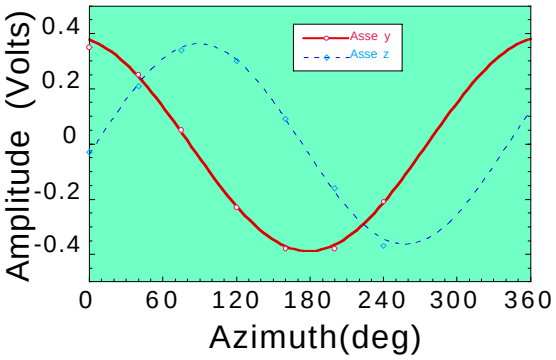

Fig.6. Output of the two axes of the low sensitivity magnetometer at different azimuth pointing directions of the gondola during the calibration procedure (see text). The plot shows the data corresponding to the axes on the horizontal plane (y and z). The curves show the result of a fit to the data with a simple sine function with amplitude and phase as free parameters.

The gondola is equipped with two magnetometers, a low sensitivity one fixed to the gondola, and a high sensitivity one that provides the required information to the on-board computer to retrieve the correct azimuth pointing. The pointing system was accurately calibrated on site before the flight. The payload was suspended in a flight configuration and the magnetic pointing procedure was calibrated against the known geographical pointing. **Fig.6** shows the behaviour of the low resolution magnetometer along the two axes on the horizontal plane, namely *y* and *z* . We point out that magnetic perturbations on the on-board magnetometers due to changes in the surrounding distribution of residual magnetic masses can arise from changes in the zenith position. Therefore, the calibration was carried out by varying the azimuth of the gondola and, for a fixed azimuth, by scanning the zenith over the range of interest. The result of these measurements are summarised in **Fig.7** where the perturbation is plotted as a function of the azimuth for different zenith positions

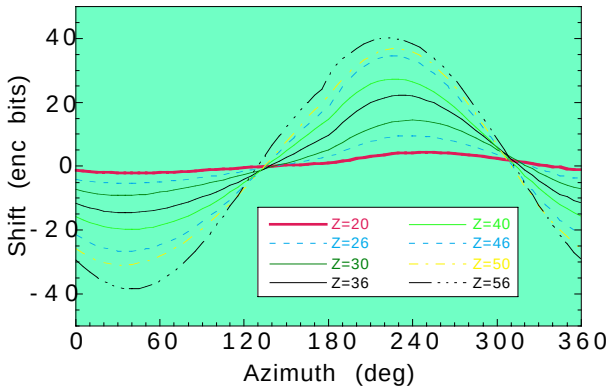

Fig.7. Perturbation in the direction of the local magnetic field as seen by the high sensitivity magnetometer located on-board of the LAPEX gondola. The perturbation is due to changes in the distribution of residual magnetic masses around the magnetometer arising from changes in the zenith position of the detector. The perturbation is plotted in steps of the 16-bits encoder used to read the output of the magnetometer.

4. Flight history

The LAPEX experiment has been flown on 6 October 1995 from the base of the NSBF-NASA Facility located at Fort Sumner, New Mexico, USA (Lat.: 34:29.4 Long.: 104:13.1 W). The flight started at 15.00 UT (9.00 am local time) and was terminated after fourteen hours at 5.00 UT (11.00 pm local time). The custom developed ground support equipment [4] allowed us to follow the main parameters of

the balloon during the flight. This information is summarised by the plots shown in Fig.8 to Fig.11 where the trajectory, the altitude, the local air temperature and the air pressure are reported as a function of the universal time.

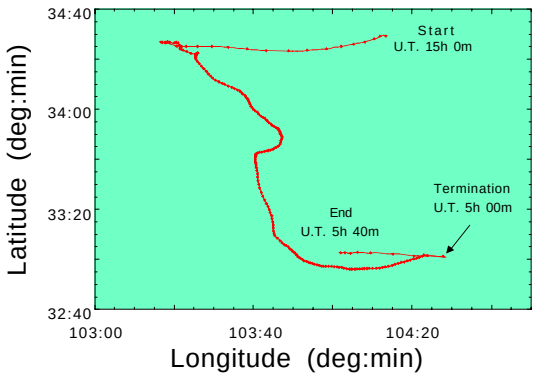

Fig.8 Trajectory of the LAPEX gondola in the latitude - longitude frame. The whole flight duration from start to termination was approximately fourteen hours with approximately eleven hours of flight at floating altitude.

The trajectory (see Fig.8) was monitored on-line using global positioning system (GPS) that allowed the position of the gondola to be determined with a sub-meter accuracy. The altitude of the gondola, as obtained by the GPS data is shown in **Fig.9** as a function of time.

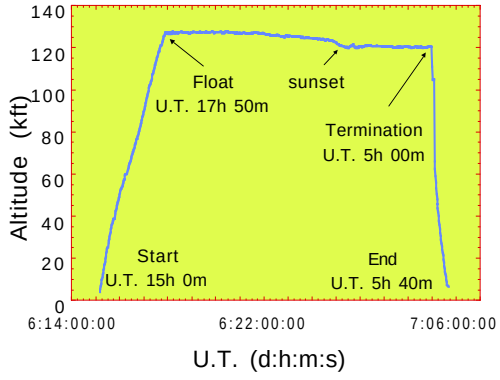

Fig.9. Balloon altitude as obtained by the on-board GPS system as a function of universal time.

Approximately three hours after launch, i.e. at 18.00 hrs (U.T.) the payload reached the float altitude of 125 kft (≈40 km). The pressure as a function of time is shown in **Fig.10.**

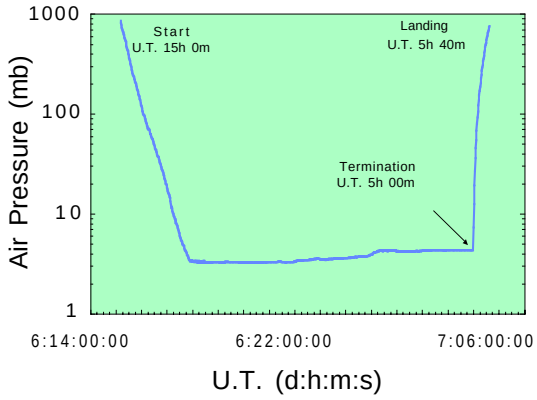

Fig.10 Air pressure as a function of time. The residual pressure at float altitude was approximately 3mb during day time and between 4 and 5mb after sunset.

According to this plot, the residual pressure at float is between 3 and 4 mB. The temperature as measured by an external probe is plotted in **Fig.11** as a function of time. After a rapid decrease during ascent, the external temperature settles when the float altitude is reached.

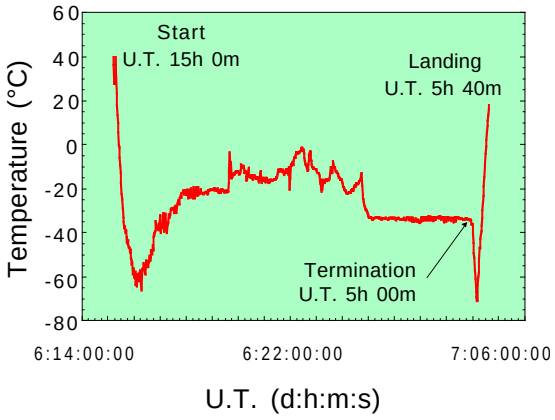

Fig.11 External air temperature as a function of time. Note that the float altitude of approximately 125 kft (40 km) is reached at 18:00 hrs (U.T.).

During day time the average temperature is approximately -15°C with fluctuations (s.d.) of 5°C due to solar irradiation effects. After sunset, at approximately 1:00 hrs (U.T.), the temperature decreases rapidly and stabilises around at an average of -35 °C with fluctuations (s.d.) within 1°C.

5. Pointing performance

The key issue in the pointing performance of the system is the accuracy of the azimuthal motion. The azimuthal pointing performance during the flight has been evaluated using the on-board star-sensor which operated in a passive mode (no feed-back in the pointing loop). The video signal of the star-sensor was recorded during the flight. In particular, a test optical source (Deneb, see observation schedule - next section) was tracked for approximately 3 minutes. The entire field of view of the star-sensor was approximately 40 arcmin. Fig.12(left) shows a star sensor image obtained during tracking and Fig.12(right) shows the result of the average of all the images acquired over one minute of tracking. According to these images, the motion of the tracked star was less than ±2 arcmin.

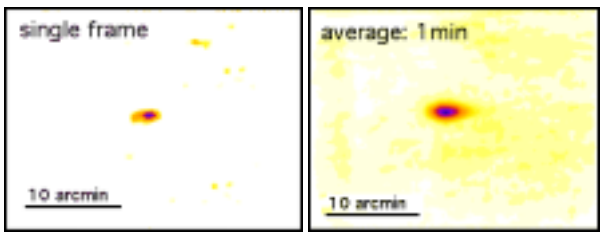

Fig.12 Star-sensor image of the test star (Deneb) for a single frame exposure (left) and averaged over 1min of exposure during tracking.

This measurement can be compared with the value obtained the signal of the magnetometer as shown in Fig.13. The result of this measurement again shows that the pointing accuracy of the LAPEX azimuthal system is accurate within ±2 arcmin.

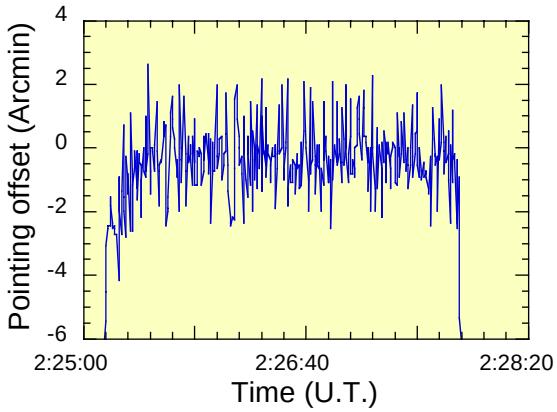

Fig.13 Magnetometer signal during the tracking of an optical source (Deneb). The pointing accuracy is within ±2 arcmin. This value is also found from a direct observation of the fluctuation of the star position as recorded by the star- sensor.

6. Observation schedule

The list of the sources observed during the flight is reported in Table.III where the universal time of each observation is also reported. Notice that the observation altitude is reached at approximately 17.00 hours (U.T.) and the observation of the first actual X-ray source starts at 17.26 hours (U.T.).

LOCAL TIME	UNIVERSAL TIME	SOURCE
9:10	15.10	START
10:50	16.50	SUN
11:26	17.26	MKN463
13.36	19.36	NGC4151
15.56	21.56	SUN
16.06	22.06	MKN463
17.07	23.07	CYG X-3
19.56	1.56	CYG X-1
20.20	2:20	DENEB
20.26	2.26	GROJ2057+43
22.47	4:47	END

Table.III. List of the sources observed by the LAPEX detection unit during the 1995 flight. Initially, during the balloon ascent phase, the sun was pointed in order to check the calibration of the pointing system. The actual observation time starts at 17.26 (U.T.) with the source MKN463.

The detector was enabled since the beginning of the flight and the count rate of each detection unit was recorded even before the actual observation time. Therefore, the performance of the whole system could be monitored by recording the changes in the environmental radioactivity (background) as a function of the altitude of the balloon.

The plot of **Fig.14** shows the count rate, integrated over the whole spectral range of the detector (20-300keV) of one of the 16 units, as a function of time (U.T.) during the whole flight. A strong increase of the background activity is clearly visible during the ascent of the balloon and stabilises around 30 counts/sec at float altitude, where observation occurs. It is worth to point out that the observation of the sources is carried out following a pre-defined scheme according to which, half of the 16 detection units are in the *on* position, that is, they look at the source, while the remaining 8 are set in an *off* position, that is, the collimators are oriented so that they look far enough (8 degrees) from the source, in order to give a simultaneous measurement of the background. After a given time interval, the configuration is reversed and the units that were in *on* configuration go in *off* and vice-versa. This procedure is repeated during the whole observation and, during the analysis of the data, the background is then subtracted from the source data.

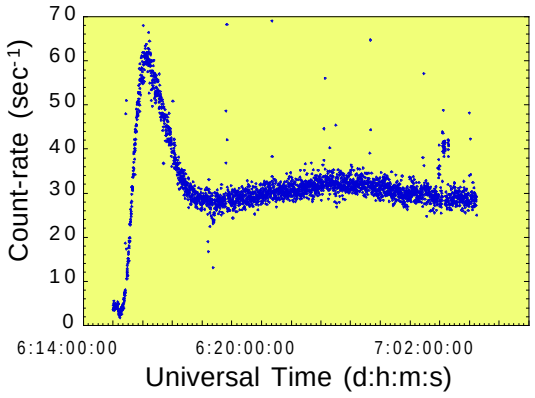

Fig.14. Count rate, integrated over the whole spectral range, of one of the 16 units of the detector as recorded during the whole flight. The rapid increase at the beginning of the flight is due to the increase of the atmospheric background activity that stabilises around 30 counts/sec at the float altitude.

The effect of the *on-off* observation procedure on the measured count rate is clearly visible in the plot of **Fig.15**, where a portion of the plot of Fig.14 concerning the observation of Cyg X-1 (see Table.III) is magnified. The corresponding portion relative to another unit set with a phase difference of half a cycle is also plotted in the same graph to show the synchronisation of the units with each other.

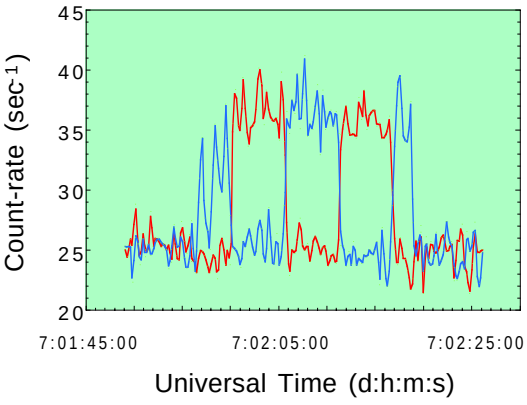

Fig.15. Count rate, integrated over the whole spectral range, of two of the 16 units of the detector as recorded during the observation of Cyg X-1. The plot shows the effect of the *on-off* observing procedure adopted to account for the background noise (see text).

7. Conclusions and future work

The analysis of the subsystems of the LAPEX experiment shows that a pointing accuracy and stability within ±2 arcmin was achieved as confirmed by magnetometer data and by the star sensor. This is an excellent starting point for the next balloon gondola (HiPeG) which we are now developing. Following the LAPEX experience, the main emphasis in the HiPeG project will be on the azimuth pointing system which will be based upon a multi-antenna GPS system and will make use of reaction wheels for higher accuracy pointing. Also, a new star sensor will be developed which be included in the pointing control loop to reach the sub-arcmin level.

References

[1] P. Laporte et al, *CLAIRE ? towards the first light for a gamma-ray lens,* Nucl. Instr. and Meth. A 442 (2000) 438.

[2] S.Silvestri, A. Basili, G. Di Cocco, T.Franceschini , F. Frontera*, L.A.Gizzi, G. Landini, *HiPeG:A pointing and stabilization system for hard-x-ray telescopes with focusing optics,*GIFCO Meeting, Italy (1999).

[3] S. Silvestri, *Ground support equipment for on-line control and monitoring of the Lapex balloon experiment,*1 st. Symposion on Stratospheric Balloons 6-7 oct. 1994 Huelva (Spain).

[4] F.Frontera et al, *Large-Area Phoswich Balloon Experiment for Hard-X-Ray Atronomy,* Il Nuovo Cimento Vol. 7C, N° 6, 1984.